



INDIAN INSTITUTE OF TECHNOLOGY MADRAS

Control of Ball Balancing Robot

Course: ME4010 Control Systems

Professor: Dr. Manish Anand

Authors:

T. Abhinand (ME23B208)

System Modeling

1 System Description

The system consists of a ball balancing robot modeled with three degrees of freedom. The mechanical structure is defined by the interaction between the wheel, the robot body, and a balancing mass.

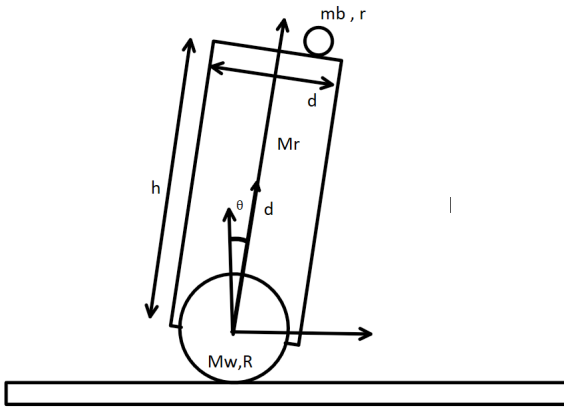


Figure 1: Diagram of the Ball Balancing Robot System

Symbol	Description
$x_w(t)$	Linear displacement of the wheel/cart
$\theta(t)$	Tilt angle of the robot body
$x(t)$	Position of the balancing mass
M_w, I_w	Mass and Inertia of the wheel
M_r, I_r	Mass and Inertia of the robot body
m_b, I_b	Mass and Inertia of the balancing mass
R	Radius of the wheel
r	Radius of the balancing mass mechanism
d	Distance to the robot body center of mass
h	Height parameter for the balancing mass
g	Gravitational acceleration

Table 1: System Parameters

2 Equations of Motion Derivation

The equations of motion are derived using the Euler-Lagrange method. The Lagrangian \mathcal{L} is defined as the difference between the total kinetic energy (T) and the total potential energy (U) of the system.

2.1 Kinetic Energy (T)

The total kinetic energy is the sum of the kinetic energies of the wheel (T_w), the robot body (T_r), and the balancing mass (T_b).

$$T_w = \frac{1}{2}M_w \dot{x}_w^2 + \frac{1}{2}I_w \left(\frac{\dot{x}_w}{R} \right)^2 \quad (1)$$

$$T_r = \frac{1}{2}M_r \dot{x}_w^2 + \frac{1}{2}I_r \dot{\theta}^2 \quad (2)$$

The kinetic energy of the balancing mass T_b includes both translational and rotational components, accounting for the relative motion $x(t)$ and the body angle $\theta(t)$:

$$T_b = \frac{1}{2}m_b(v_{b,x}^2 + v_{b,y}^2) + \frac{1}{2}I_b \left(\frac{\dot{x}}{r} \right)^2 \quad (3)$$

2.2 Position and Velocity Analysis

The position of the balancing mass in the inertial frame is derived by first expressing its position in the body-fixed frame, then applying a rotation and translation.

2.2.1 Body-Fixed Coordinates

In the body-fixed frame, the position of the balancing mass relative to the body center is:

$$\begin{bmatrix} x_{rel} \\ y_{rel} \end{bmatrix} = \begin{bmatrix} x \\ h+r \end{bmatrix} \quad (4)$$

2.2.2 Rotation Matrix

The rotation from the body-fixed frame to the inertial frame is represented by the rotation matrix:

$$\mathbf{R}(\theta) = \begin{bmatrix} \cos(\theta) & \sin(\theta) \\ -\sin(\theta) & \cos(\theta) \end{bmatrix} \quad (5)$$

where θ is the tilt angle of the robot body.

2.2.3 Inertial Position Derivation

The position of the balancing mass in the inertial frame is obtained by rotating the body-fixed coordinates and adding the wheel position offset:

Performing the matrix multiplication:

$$\begin{bmatrix} x_b \\ y_b \end{bmatrix} = \begin{bmatrix} \cos(\theta) & \sin(\theta) \\ -\sin(\theta) & \cos(\theta) \end{bmatrix} \begin{bmatrix} x \\ h+r \end{bmatrix} + \begin{bmatrix} x_w \\ 0 \end{bmatrix} \quad (6)$$

Expanding the matrix product:

$$x_b = \cos(\theta) \cdot x + \sin(\theta) \cdot (h+r) + x_w \quad (7)$$

$$y_b = -\sin(\theta) \cdot x + \cos(\theta) \cdot (h+r) \quad (8)$$

Rearranging:

$$x_b = x \cos(\theta) + (h+r) \sin(\theta) + x_w \quad (9)$$

$$y_b = (h+r) \cos(\theta) - x \sin(\theta) \quad (10)$$

2.3 Potential Energy (U)

The total potential energy is the sum of the potential energies of the components:

$$U = U_b + U_r + U_w \quad (11)$$

where:

$$U_b = m_b g ((h+r) \cos(\theta) - x \sin(\theta)) + R + \text{const} \quad (12)$$

$$U_r = M_r g d \cos(\theta) + R \quad (13)$$

$$U_w = R \quad (\text{constant}) \quad (14)$$

2.4 Lagrangian

The Lagrangian of the system is given by:

$$\mathcal{L} = T - U \quad (15)$$

2.5 Equations of Motion

Applying the Euler-Lagrange equation:

$$\frac{d}{dt} \left(\frac{\partial \mathcal{L}}{\partial \dot{q}_i} \right) - \frac{\partial \mathcal{L}}{\partial q_i} = 0 \quad (16)$$

for the generalized coordinates $q = [x_w, \theta, x]$, we obtain the three equations of motion.

3 State-Space Formulation

3.1 Mass Matrix

The system dynamics can be expressed in the form:

$$\mathbf{M}(\mathbf{q})\ddot{\mathbf{q}} + \mathbf{K}(\mathbf{q}, \dot{\mathbf{q}}) = 0 \quad (17)$$

The mass/inertia matrix \mathbf{M}_1 is:

$$\mathbf{M}_1 = \begin{bmatrix} \frac{I_b}{r^2} + m_b & m_b(h+r) \\ m_b(h+r) & I_r + m_b(h+r)^2 \end{bmatrix} \quad (18)$$

3.2 Stiffness Matrix

The stiffness/restoring force matrix \mathbf{M}_2 captures the gravitational restoring terms:

$$\mathbf{M}_2 = \begin{bmatrix} 0 & gm_b \\ gm_b & g(M_r d + m_b(h+r)) \end{bmatrix} \quad (19)$$

3.3 Input Coupling Matrix

The torque/input coupling matrix \mathbf{M}_3 represents the effect of the motor torque on the generalized coordinates:

$$\mathbf{M}_3 = \begin{bmatrix} -m_b(h+r) \\ -I_r - m_b(h+r)^2 \end{bmatrix} \quad (15)$$

3.4 Linearized State-Space Matrices

The system can be linearized around the equilibrium point $\theta = 0$ to obtain the linear state-space representation. Define the state vector as:

$$\mathbf{x} = \begin{bmatrix} x \\ \theta \\ \dot{x} \\ \dot{\theta} \end{bmatrix} \quad (16)$$

The linearized state-space dynamics are:

$$\dot{\mathbf{x}} = \mathbf{A}\mathbf{x} + \mathbf{B}u \quad (17)$$

where the state transition matrix \mathbf{A} is:

$$\mathbf{A} = \begin{bmatrix} 0 & 1 & 0 & 0 \\ A_1(1,1) & 0 & A_1(1,2) & 0 \\ 0 & 0 & 0 & 1 \\ A_1(2,1) & 0 & A_1(2,2) & 0 \end{bmatrix} \quad (18)$$

and the input matrix \mathbf{B} is:

$$\mathbf{B} = \begin{bmatrix} 0 \\ B_1(1) \\ 0 \\ B_1(2) \end{bmatrix} \quad (24)$$

where $\mathbf{A}_1 = -\mathbf{M}_1^{-1}\mathbf{M}_2$ and $\mathbf{B}_1 = \mathbf{M}_1^{-1}\mathbf{M}_3$.

The output equation is:

$$y = \mathbf{C}\mathbf{x} + \mathbf{D}u \quad (25)$$

where $\mathbf{C} = [0 \ 0 \ 1 \ 0]$ and $\mathbf{D} = 0$.

Control and State Estimation

Dimension	Value	Units
M_w	4.3	kg
M_r	10.12	kg
m_b	0.00271	kg
I_w	0.2725	kg · m ²
I_r	0.4747	kg · m ²
I_b	1.740×10^{-6}	kg · m ²
R	0.356	m
r	0.04006	m
d	0.18865	m
h	0.31665	m
g	9.81	m/s ²

Table 2: Numerical Parameters for the Ball Balancing Robot System

4 Numerical State-Space Model

Using the parameters, the linearized state-space model $\dot{\mathbf{x}} = \mathbf{Ax} + \mathbf{Bu}$, $y = \mathbf{Cx} + \mathbf{Du}$ is evaluated numerically as:

$$\mathbf{A} = \begin{bmatrix} 0 & 1.0000 & 0 & 0 \\ -0.0143 & 0 & -3.0441 & 0 \\ 0 & 0 & 0 & 1.0000 \\ 0.0560 & 0 & 39.4486 & 0 \end{bmatrix} \quad (26)$$

$$\mathbf{B} = \begin{bmatrix} 0 \\ 0 \\ 0 \\ 1 \end{bmatrix} \quad (27)$$

$$\mathbf{C} = [0 \ 0 \ 1 \ 0], \quad \mathbf{D} = 0 \quad (28)$$

5 LQR Controller Design

5.1 Optimal Control Problem

The Linear Quadratic Regulator (LQR) is designed to stabilize the unstable ball balancing robot while minimizing a cost function:

$$J = \int_0^\infty (\mathbf{x}^T \mathbf{Q} \mathbf{x} + \mathbf{u}^T \mathbf{R} \mathbf{u}) dt \quad (19)$$

5.2 Bryson's Rule for Weight Selection

$$\mathbf{Q} = \text{diag} \left[\frac{1}{x_{\max}^2}, \frac{1}{\dot{x}_{\max}^2}, \frac{1}{\theta_{\max}^2}, \frac{1}{\dot{\theta}_{\max}^2} \right], \quad \mathbf{R} = \frac{1}{u_{\max}^2} \quad (20)$$

$$x_{\max} = d/8 = 0.0236 \text{ m}$$

$$\dot{x}_{\max} = 0.5 \text{ m/s}$$

$$\theta_{\max} = 15^\circ = 0.2618 \text{ rad}$$

$$\dot{\theta}_{\max} = 2 \text{ rad/s}$$

$$u_{\max} = 5 \text{ (actuator units)}$$

5.3 Optimal Feedback Control Law

$$\mathbf{A}^T \mathbf{S} + \mathbf{S} \mathbf{A} - \mathbf{S} \mathbf{B} \mathbf{R}^{-1} \mathbf{B}^T \mathbf{S} + \mathbf{Q} = 0 \quad (21)$$

$$\mathbf{K} = \mathbf{R}^{-1} \mathbf{B}^T \mathbf{S}, \quad u = -\mathbf{K} \mathbf{x} \quad (22)$$

5.4 Closed-Loop System

$$\dot{\mathbf{x}} = (\mathbf{A} - \mathbf{B}\mathbf{K})\mathbf{x} = \mathbf{A}_{cl}\mathbf{x} \quad (23)$$

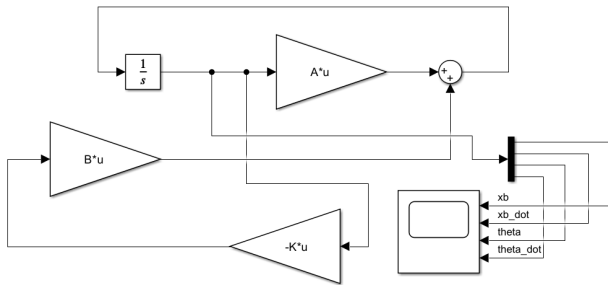


Figure 2: LQR Controller (simulink)

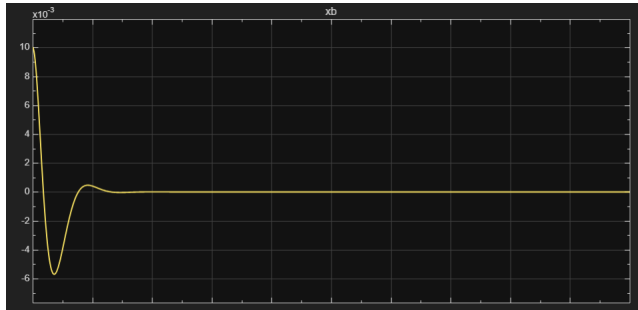


Figure 3: LQR Controller (xb plot)

6 State Estimation

6.1 Observability Analysis

$$\mathbf{O} = \begin{bmatrix} \mathbf{C} \\ \mathbf{CA} \\ \mathbf{CA}^2 \\ \mathbf{CA}^3 \end{bmatrix} \quad (24)$$

For fully observable, system rank(O) = 4.

7 Full-Order Kalman Observer

7.1 Observer Dynamics

$$\dot{\hat{\mathbf{x}}} = \mathbf{A}\hat{\mathbf{x}} + \mathbf{B}u + \mathbf{L}(y - \mathbf{C}\hat{\mathbf{x}}) \quad (25)$$

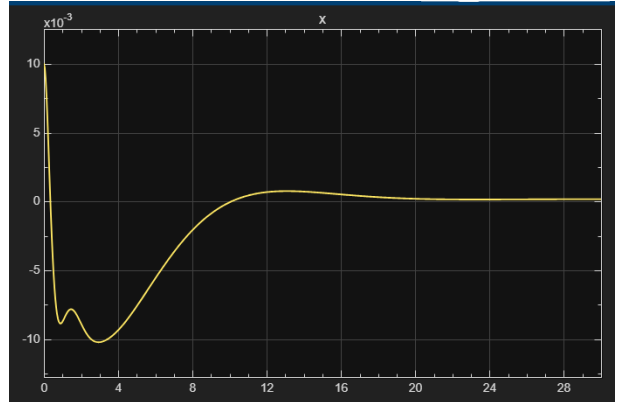
7.2 Kalman Filter Gain Design

$$\mathbf{Q}_{obs} = 0.1 \cdot \text{diag}[10^7, 100, 10^6, 10], \quad \mathbf{R}_{obs} = 0.00001 \quad (26)$$

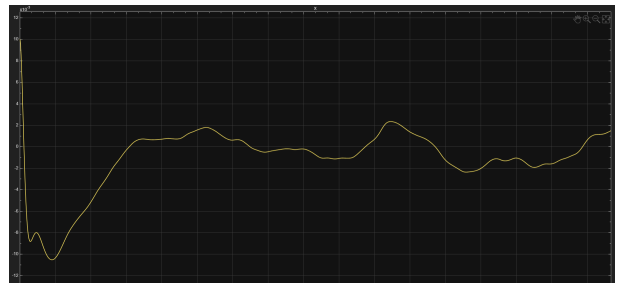
$$\mathbf{L} = \mathbf{P}\mathbf{C}^T \mathbf{R}_{obs}^{-1} \quad (27)$$

7.3 Estimation Error Dynamics

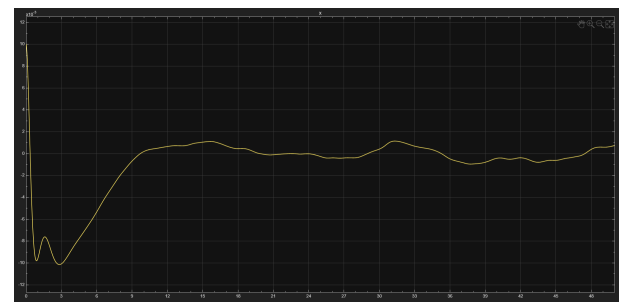
$$\dot{\mathbf{e}} = (\mathbf{A} - \mathbf{LC})\mathbf{e} \quad (28)$$



(a) No noise (xb plot)



(b) Measurement noise (xb plot)



(c) Noise filtered

Figure 4: Full-order observer responses

8 Minimum-Order(Reduced-Order) Observer

8.1 Motivation

Since θ is directly measured, a minimum-order observer estimates only unmeasured states $\dot{x}, x, \dot{\theta}$.

8.2 State Partitioning

$$\mathbf{x}_a = [\theta], \quad \mathbf{x}_b = \begin{bmatrix} x \\ \dot{x} \\ \dot{\theta} \end{bmatrix} \quad (29)$$

$$\begin{bmatrix} \dot{\mathbf{x}}_a \\ \dot{\mathbf{x}}_b \end{bmatrix} = \begin{bmatrix} \mathbf{A}_{aa} & \mathbf{A}_{ab} \\ \mathbf{A}_{ba} & \mathbf{A}_{bb} \end{bmatrix} \begin{bmatrix} \mathbf{x}_a \\ \mathbf{x}_b \end{bmatrix} + \begin{bmatrix} \mathbf{B}_a \\ \mathbf{B}_b \end{bmatrix} u \quad (30)$$

8.3 Reduced-Order Observer

$$\begin{aligned} \dot{\mathbf{z}} &= \mathbf{A}_{bb}\mathbf{z} + \mathbf{A}_{ba}\mathbf{x}_a + \mathbf{B}_b u + \\ \mathbf{K}_{min}(\mathbf{x}_a - \mathbf{A}_{aa}\mathbf{x}_a - \mathbf{A}_{ab}\mathbf{z} - \mathbf{B}_a u) \end{aligned} \quad (31)$$

$$\hat{\mathbf{x}}_b = \mathbf{z} + \mathbf{K}_{min}\mathbf{x}_a \quad (32)$$

8.4 Noise Covariances

$$\mathbf{Q}_{min} = 10000 \cdot \text{diag}[1, 100, 1], \quad \mathbf{R}_{min} = 0.005 \quad (33)$$

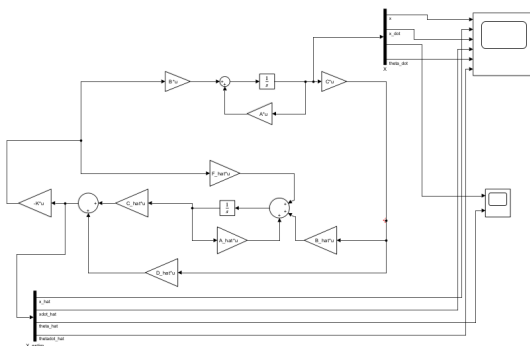


Figure 5: Minimum-Order Observer (simulink)

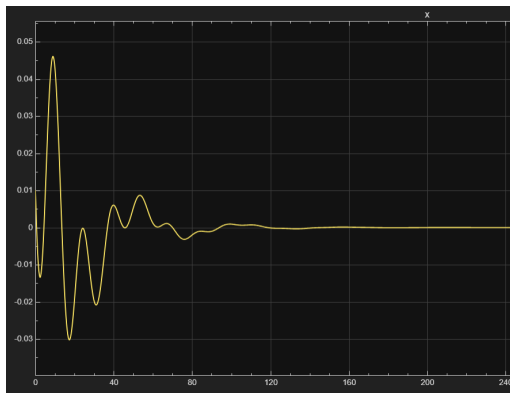


Figure 6: Minimum-Order Observer ($\hat{\mathbf{x}}_b$)

9 Minimum-Order Observer with Noise Filtering

9.1 Motivation for Filtering

Measurement noise on θ can degrade observer performance. A low-pass filter is applied to the measured angle before feeding it to the minimum-order observer.

9.2 First-Order Low-Pass Filter (14 Hz)

A first-order low-pass filter is implemented with cutoff frequency $f_c = 14$ Hz:

$$\tau = \frac{1}{2\pi f_c} = \frac{1}{2\pi \cdot 14} \approx 0.01137 \text{ s} \quad (34)$$

The filter transfer function is:

$$H(s) = \frac{1}{\tau s + 1} = \frac{1}{0.01137s + 1} \quad (35)$$

The filtered measurement y_{filt} is obtained from:

$$\dot{y}_{filt} = -\frac{1}{\tau}(y_{filt} - y_{meas}) \quad (36)$$

or in discrete form:

$$y_{filt}(k+1) = y_{filt}(k) + \frac{\Delta t}{\tau} (y_{meas}(k) - y_{filt}(k)) \quad (37)$$

9.3 Butterworth Filter (14 Hz)

For a second-order Butterworth filter:

$$H(s) = \frac{\omega_n^2}{s^2 + \sqrt{2}\omega_n s + \omega_n^2} \quad (38)$$

with

$$\omega_n = 2\pi f_c = 2\pi \cdot 14 \approx 87.96 \text{ rad/s} \quad (39)$$

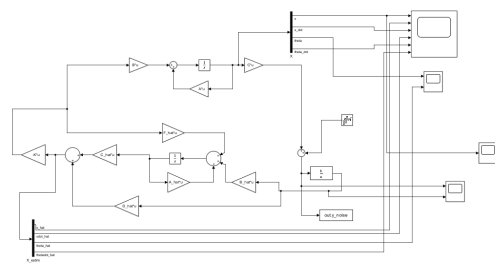


Figure 7: Minimum-Order Observer filtered (simulink)

9.4 Integrated Observation Architecture

$$\begin{aligned} \dot{\mathbf{z}} &= \mathbf{A}_{bb}\mathbf{z} + \mathbf{A}_{ba}y_{filt} + \mathbf{B}_b u \\ &+ \mathbf{K}_{min}(y_{filt} - \mathbf{A}_{aa}y_{filt} - \mathbf{A}_{ab}\mathbf{z} - \mathbf{B}_a u) \end{aligned} \quad (40)$$

10 Integrated Control-Observer System

10.1 Separation Principle

$$u = -\mathbf{K}\hat{\mathbf{x}} \quad (41)$$

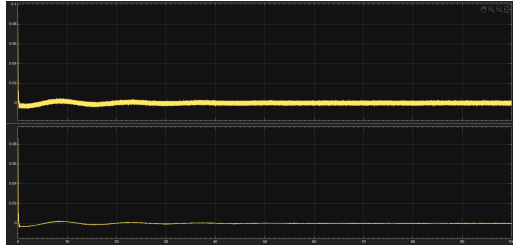


Figure 8: Minimum-Order Observer (measurement noise filtering)

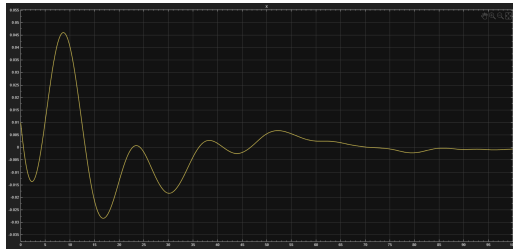


Figure 9: Minimum-Order Observer filtered (\hat{x}_b)

10.2 Combined Closed-Loop Dynamics

$$\begin{bmatrix} \dot{\mathbf{x}} \\ \dot{\mathbf{e}} \end{bmatrix} = \begin{bmatrix} \mathbf{A} - \mathbf{B}\mathbf{K} & \mathbf{B}\mathbf{K} \\ 0 & \mathbf{A} - \mathbf{L}\mathbf{C} \end{bmatrix} \begin{bmatrix} \mathbf{x} \\ \mathbf{e} \end{bmatrix} \quad (42)$$

11 Summary of Observer Architectures

The key characteristics of the observer architectures are summarized below:

- **Full-Order Kalman Observer**

Order: 4

States Estimated: All ($\mathbf{x} = [x, \theta, \dot{x}, \dot{\theta}]^T$)

Advantages: Provides complete state information; is the standard implementation.

- **Reduced-Order Observer**

Order: 3

States Estimated: $\dot{x}, x, \dot{\theta}$ (unmeasured states)

Advantages: Offers better computational efficiency with less redundancy.

- **Reduced with Filter Observer**

Order: 3

States Estimated: Filtered θ plus unmeasured states

Advantages: Noise rejection capability, leading to smooth estimates.

12 Root locus method: PID

12.1 Cascade Control Strategy

In addition to State-Space methods, a classical Cascade PID control architecture was designed using Root Locus techniques. This approach decomposes the unstable system into two loops:

1. **Inner Loop (Stabilization):** Controls the tilt angle θ to maintain upright stability. This loop must have faster dynamics.

2. **Outer Loop (Position):** Controls the ball position x . The output of this controller serves as the reference angle θ_{ref} for the inner loop.

12.2 Inner Loop Design (θ)

The plant transfer function from input torque to angle $G_\theta(s)$ has a pair of Real axis poles (one stable, one unstable) and a pair of imaginary poles. A PID controller $C_\theta(s)$ is tuned to stabilize the system:

$$C_\theta(s) = K_{p,\theta} + \frac{K_{i,\theta}}{s} + K_{d,\theta}s \quad (43)$$

Based on the tuning parameters:

$$K_{p,\theta} = 3000, \quad K_{i,\theta} = 10, \quad K_{d,\theta} = 25 \quad (44)$$

The closed-loop inner system ensures all poles are in the Left Half Plane (LHP), guaranteeing stability for the pendulum dynamics.

12.3 Outer Loop Design (x)

The Outer loop regulates the position x by manipulating the setpoint of the inner loop (θ_{ref}). The controller $C_x(s)$ is defined as:

$$C_x(s) = K_{p,x} + \frac{K_{i,x}}{s} + K_{d,x}s \quad (45)$$

Using Root Locus analysis on the effective plant $G_x(s)$ (from $\theta_{ref} \rightarrow x$), the gains were selected to ensure tracking performance while maintaining stability boundaries:

$$K_{p,x} = 5.0, \quad K_{i,x} = 0.01, \quad K_{d,x} = 41 \quad (46)$$

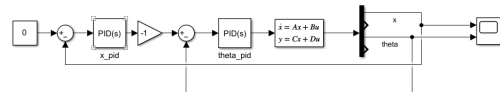


Figure 10: PID controller (simulink diagram)

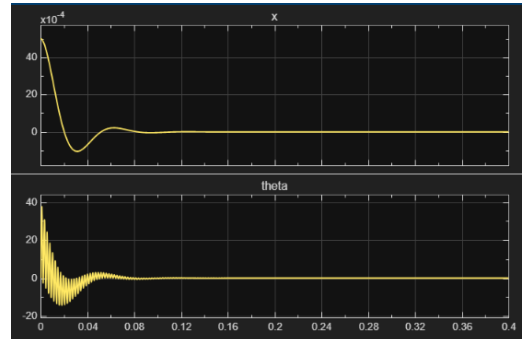


Figure 11: PID controller (simulink plot)

13 Performance Comparison (settling time)

Control Architecture	Settling Time (T_s)
PID (Cascade)	84.45 s
LQR (State Feedback)	4.77 s
LQR + Full Obs.	31.56 s
LQR + Reduced Obs.	138.92 s

Table 3: Comparison of Settling Times

[Github link to project](#)